Preprints, Ninth Conference on Numerical Weather Prediction, Denver, C0, Oct. 10-15,
American Meteorological Society, 430-433.

INITIALIZATION AND ASSIMILATION OF CLOUD AND RAINWATER IN A REGIONAL MODEL

William H. Raymond and William S. Olson
Cooperative Institute for Meteorological Satellite Studies
The University of Wisconsin
Madison, Wisconsin 53706

1. INTRODUCTION

In this study we examine the initialization and assimilation of cloud and rainwater quantities in a mesoscale regional model. In our study forecasts of explicit cloud and rainwater are made using conservation equations. The physical processes include condensation, evaporation, autoconversion, accretion and the removal of rainwater by fallout. These physical processes, some of which are parameterized, represent source and sink terms in the conservation equations. The question of how to initialize the explicit liquid water calculations in numerical models and how to retain information about precipitation processes during the 4-D assimilation cycle are important issues that will be addressed.

With increasing computer speed there has been a slow but study enhancement in model horizontal grid resolution. Current NWP models are approaching the spatial resolution where time-dependent cloud variables are physically relevant. In our pilot study we examine the feasibility of initializing and assimilating cloud and rainwater using explicit cloud conservation equations within a regional mesoscale model. The knowledge of cloud and rainwater fields as a function of time and space provides information, such as model heating rates and vertical distributions, that are more difficult to obtain from conventional cloud parameterization approaches where cloud properties are not retained from one time step to the next. Global models will soon routinely solve explicit cloud and rainwater conservation equations, but limited area mesoscale models can be utilized to examine this topic now.

Cloud and rainwater are the cumulative products of the transport of atmospheric moisture, both vapor and liquid, plus the physical processes included in cloud development and decay. By their very nature cumulative processes are difficult to initiate in numerical models, and it is common for precipitation to be absent during the first few hours of a numerical forecast. One reason for this deficiency is the resolution of the data. Conventional surface and upper air reports are known not to capture the mesoscale circulations that have the enhanced convergence necessary to support mesoscale precipitation processes. The missing mesoscale circulations also influence the moisture and thermal fields (Turpeinen 1990). Consequently, in order to initiate precipitation and assimilate cloud parameters it is necessary to know additional information beyond the conventional synoptic data base. This might include accurate estimates of the vertical heating rates and the low level convergence and/or the high level divergence that produces the cloud-sustaining vertical motion field. Also, model generated inaccuracies or shortcomings, e.g., phase errors and inadequate physics, must be accommodated in some manner.

When the heating rates are known or can be approximated, then either diabatic or cumulus initialization is possible (Errico and Rasch 1988; Donner 1988). These initialization procedures help establish circulation patterns consistent with latent heating processes that are otherwise not resolved in synoptic scale data. For a review of recent studies using diabatic initialization schemes, see Table 1 in Turpeinen et al. (1990). Without the heating rate information each forecast must go through a short time period where the precipitation processes must 'spin-up' before rainfall can be produced. In regional mesoscale models this spin-up usually occurs during the first 2 to 6 hours. Diabatic initialization should reduce the degree and duration of the spin-up. In contrast, normal mode or dynamic initialization procedures, designed to help with the removal of gravity waves during initialization, only provide slight or no assistance in speeding up precipitation processes (Lejenas 1980).

Cloudwater and rainwater data are generally not available. Rain gauge reports imply information about the total amount of liquid water reaching the surface, but no knowledge about the instantaneous vertical distribution is recoverable. Most microwave satellite measurements of instantaneous cloud quantities only resolve the vertically integrated cloud and/or integrated rainwater. Thus it is necessary to make some assumption about the vertical distribution of the heating rate. New physical retrieval methods that combine observed microwave satellite radiances with known meteorological fields and/or physical constraints should provide some insight into the vertical partitioning of the liquid water. These techniques are just beginning to be examined.

The use of diabatic initialization requires an answer to the question of how the latent heating is going to be distributed in the vertical. Some studies have used representative profiles (Fiorino and Warner 1981); others assume a general parabolic profile (Tarbell et al 1981; Salmon and Warner 1986, etc.) while some have tried to use the forecast model itself in some fashion (Wergen 1988: Danard 1985: Turpeinen et al. 1990). Donner (1988) used a variational formulation to optimize the vertical distribution with respect to the methodology of the Kuo cumulus parameterization. In all but the Donner study it has been

customary to use either the diabatic omega equation or a diabatic form of the normal mode initialization scheme. Earlier pioneering work by Krishnamurti et al. (1984) suggested that a reanalysis of the moisture and wind field is also needed.

In this study we will incorporate in the initialization the heating rates, cloudwater, and rainwater predicted by a forecast beginning 12 hours before the assimilation process. This information will be combined with new information from observations, and heating rates will be utilized in a diabatic form of the vertical mode initialization scheme of Bourke and McGregor (1983). Theoretically, if data is always available then cloud and rainwater could be treated much like other meteorological variables, i.e., updated and modified during the 4D assimilation process. Caution is however required when making large changes to existing model cloud fields, or to the dynamics that support the precipitation process. Testing and experience with explicit cloud initialization will dictate what the correct procedure should be.

Results from only a few experiments are presented here. An evaluation of the contribution of the satellite data will be given at the conference.

2. MODELING CONSIDERATIONS

A modified version of the Bureau of Meteorology Research Centre (BMRC) operational incremental O/I analysis (Mills and Seaman 1990), vertical mode initialization or VMI (Bourke and McGregor 1983), and semi-implicit forecast model (Leslie, et al. 1985) are used in this investigation. The incremental analysis is set to preserve the irrotational wind field while the rotational component of the differences between data and model guess wind and other fields are evaluated by the O/I. In our initial tests the horizontal resolution is 120 km, while the vertical sigma coordinate is subdivided into 15 levels. We selected the low resolution 120 km grid spacing on a 35x35 horizontal grid configuration to specifically examine problems that are relevant or commonly encountered in today's centers for numerical weather prediction.

In our present study the Kuo cumulus parameterization is turned off and the conventional large scale precipitation procedure is replaced with explicit conservation equations for cloudwater and rainwater. The explicit cloud physics contains processes modeled using a modified Kessler type scheme (Kessler 1974), while the condensation and fall velocity calculations are similar to that described in Anthes, et al. (1987). The 'fallout' term is calculated by a semi-Lagrangian method to allow for the 10 minute time steps used in the semi-implicit model calculations. Ice phase cloud particles have not yet been included in the model.

Part of the goal of the current study is to modify the model cloud and rainwater fields using SSM/I retrievals of integrated total liquid water or vertical distributions of water. These observed quantities will be used to perturb existing model cloud and rainwater fields. Heating rates, lagged by one time step (Δt=10 min) or based on the total liquid water from the 12h pre-forecast, are used in the initialization. Many different types of model experiments are to be conducted, including those related to the model's response to diabatic and initial information.

Because of horizontal scale considerations, our explicit cloud calculations do not model individual clouds but do approximate average values for a system or complex of clouds. This was the motivation behind the modifications made to the Kessler (1974) cloud physics formulation. It is known that the lifetime of individual clouds is less than one hour while a cloud complex exists for many hours with remnants lasting for days. Thus Kessler's accretion (collection) process was modified to slow greatly the conversion from cloud to rainwater when the cloud water C is below a preset critical value C_{crit}. Also incorporated is a vertical dependence on temperature that follows the scheme suggested by Schlesinger (1990). This latter change helps retain and enhance anvil or cloud top features. In mixing ratio units (gg^{-1}), the contribution to the rate of change from accretion is

$$ACC \equiv 0.88 C_1 C_2 \, C \, R^{0.875} \qquad (1)$$

where $C_1 = \min[\,1.0,\ 1.0 - (C_{crit} - C)/C_{crit}\,]$,

$C_2 = \min[\,1.0, (T - 233)/40\,]$,

$C_2 = \max[\,1.0, C_2\,]$.

Here R is rainwater in mixing ratio units, T is the temperature in degrees Kelvin, and C_{crit}=1 gkg^{-1}. Initial experiments give promising results, but additional tests and verifications will be made to further evaluate computed cloud water quantities. These will include comparisons between model cloud water fields and SSM/I retrievals of cloud water distributions.

To facilitate the large time step size used in the semi-implicit forecast model the fallout term in sigma coordinates is rewritten as two terms, one of which represents vertical advection,

$$g\partial(\rho v_t R)/\partial\sigma \equiv A\partial(p^* R)/\partial\sigma + (p^* R g/p^*)\partial(\rho v_t)/\partial\sigma . \qquad (2)$$

Here ρ is the air density, v_t (ms^{-1}) is the terminal velocity of raindrops, p^* is the surface pressure, g is the acceleration of gravity and A (s^{-1}) is equivalent to a velocity in the vertical σ coordinate system, that is

$$A = g\rho v_t/p^* . \qquad (3)$$

The time tendency for A using (2) now can be found by semi-Lagrangian procedures.

3. DISCUSSION OF RESULTS

Super-imposed over the GOES 7 IR image in Fig. 1 are contours of cloudwater (solid) and rainwater (dashed) for sigma level 4 (approx. 300 mb) from a 12h forecast. The contour interval is 0.1 gkg^{-1}. The initial field for this ERICA (Experiment on Rapidly Intensifying Cyclones over the Atlantic) IOP-5 case is obtained from NMC's initialized global analysis. For the most part, the forecasted cloud fields assume the horizontal comma-shape shown in the

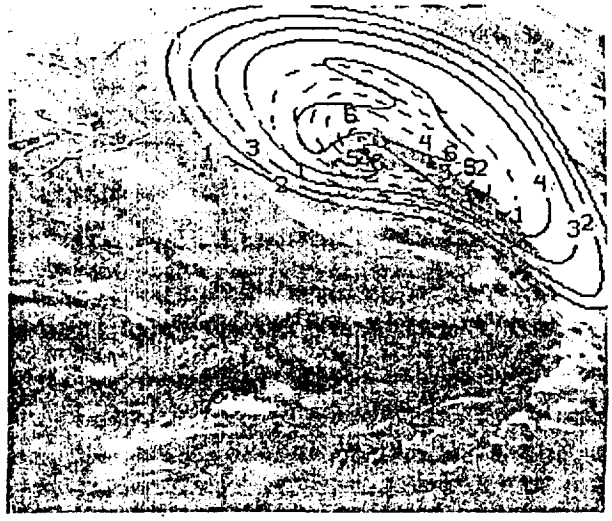

Fig. 1. Contours (0.1 gkg^{-1}) of cloudwater (solid) and rainwater (dashed) from a 12h forecast (0000 to 1200UTC, 20 Jan 1989) are superimposed over the GOES IR image.

image. In this forecast no diabatic initialization was used. When the modifications to the accretion term proposed in Eq. (1) are removed, the amount of cloud water is reduced to just one short contour (not shown) while the rainwater is enhanced slightly beyond that shown in Fig. 1. Cloudwater amounts at lower sigma levels also are much reduced when the original Kessler formulation is used. With either method the total rainfall is nearly identical in magnitude and areal coverage. The maximum rainfall over 12 hours was 33 mm for the modified approach and 34 mm for the original Kessler formulation.

In Fig. 2 the area averaged precipitation rate at each time step is plotted versus the time step for forecasts between 1200UTC, 19 Jan and 1200UTC, 20 Jan 1989. In the two forecasts without explicit clouds (labeled "large scale"), all excess water vapor exceeding saturation falls out immediately. This approach is known to produce rainfall rapidly. In contrast, note that the precipitation in the explicit

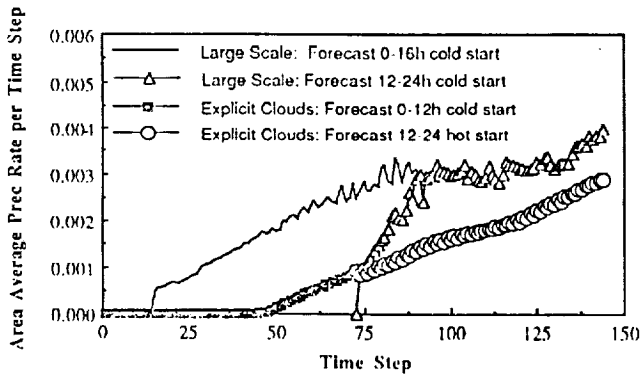

Fig. 2. Area average precipitation rate (cm) is plotted versus the time step for 4 forecasts. Forecasts with and without explicit clouds illustrate the differences in the precipitation spin-up time.

cloud calculations is delayed. This is because the autoconversion threshold, used to model the water holding capacity of clouds, is not triggered until the cloudwater exceeds 0.5 gkg^{-1}.

After 12h or 72 time steps, the forecast fields generated by the explicit cloud calculations are assimilated to begin a second 12-hour forecast. Note in Fig. 2 that the precipitation rate remains unchanged following the assimilation step as illustrated by the continuous curve between steps 72 (square) and 73 (circle). However, the precipitation rate can incur irregular behavior if the irrotational wind or dynamics are significantly changed. The incremental analysis in our assimilation preserves the irrotational wind component from the previous forecast. But, our current VMI initialization can alter the convergence and/or divergence. Thus, some consideration is being given to installing an incremental initialization procedure.

In Fig. 3 we expand the view of the second 12h period presented earlier in Fig. 2. Two of the curves from Fig. 2 are reproduced for comparison purposes. They include the cold started large scale calculations represented by the triangle curve, and the assimilated hot start shown with circles. Additionally, cold and hot started explicit cloud calculations beginning with the global initialized analysis are presented. The hot started forecasts utilize cloudwater and rainwater forecasted by the 12h pre-forecast. The heating rate at time step 72 is also used in the diabatic vertical mode initialization.

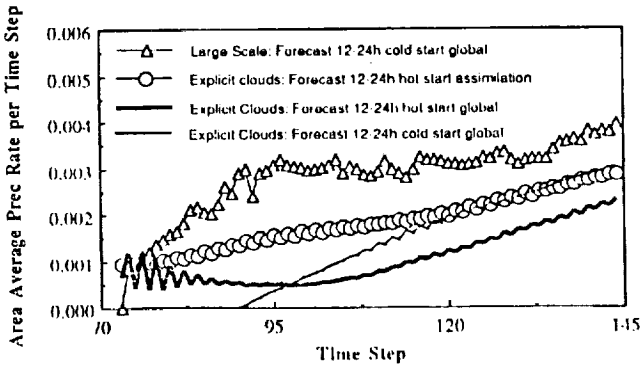

Fig. 3. Same as Fig. 2 except for initialization. All forecasts begin at time step 72.

It is clear that when the previous forecast model fields are used, as in the assimilation process, there is dynamics to support the cloud and rainwater. Thus the forecasted precipitation rate behaves properly (circle curve). When the supporting mesoscale dynamics and moisture supply are missing, as in the global initialized analysis, then adding cloud and rainwater initially can result in less realistic behavior as illustrated by the heavy solid curve in Fig. 3. This curve illustrates our worst-case scenario. For this latter case, improvement is obtained when the heating rates are also used to force or nudge the dynamics (Wang and Warner

1988) toward the desired goal (not shown). We discovered that enhanced development can become too strong in a reduced area when only the heating rates from time step 72 in the 12h pre-forecast are used. Approximating the heating rates from the total cloudwater and rainwater fields gives better results.

Many additional experiments are required before the best strategy or strategies are identified. But, the assimilation approach using incremental changes clearly is indicated to be a powerful technique that could solve the spin-up problem. However, remotely sensed cloudwater and rainwater data, and information about their vertical distribution, is still required if the forecast is to correctly simulate the atmosphere.

Acknowledgements. This work was supported by NASA Grant NAGW-1855. One author (WHR) was supported in part by National Science Foundation Grant ATM-8920508.

References

Anthes, R. A., E-Y Hsie and Y-H Kuo, 1987: Description of the Penn State/NCAR mesoscale model version 4 (MM4). NCAR Technical Note NCAR/TN-282+STR. National Center for Atmospheric Research, Boulder, Colorado, 66pp.

Bourke, W. and J. L. Mcgregor, 1983: A nonlinear vertical mode initialization scheme for a limited area prediction model. *Mon. Wea. Rev.*, **111**, 2285-2297.

Danard, M., 1985: On the use of satellite estimates of precipitation in initial analyses for numerical weather prediction. *Atmosphere-Ocean*, **23**, 23-42.

Donner, L. J., 1988: An initialization for cumulus convection in numerical weather prediction models. *Mon. Wea. Rev.*, **116**, 377-385.

Errico, R. and P. J. Rasch, 1988: A comparison of various normal-mode initialization schemes and the inclusion of diabatic processes. *Tellus*, **40A**, 1-25.

Fiorino, M and T.T. Warner, 1981: Incorporating surface winds and rainfall rates into the initialization of a mesoscale hurricane model. *Mon. Wea. Rev.*, **109**, 1914-1929.

Kessler, E., 1974: Model of precipitation and vertical air currents. *Tellus*, **26**, 519-542.

Krishnamurti, T. N., K. Ingles, S. Cocke, R. Pasch, and T. Kitade, 1984: Details of low latitude medium range weather prediction using a global spectral model II. Effect of orography and physical initialization. *J Meteor. Soc. Japan*, **62**, 613-649.

Lejenas, H., 1980: On the influence of the technique of nonlinear normal mode initialization on the nonconvective precipitation rate. *Mon. Wea. Rev.*, **108**, 1465-1468.

Leslie, L. M., G. A. Mills, L. W. Logan, D. J. Gauntlett, G. A. Kelly, J. L. McGregor and M. J. Manton, 1985: A high resolution primitive equation NWP model for operations and research. *Aust. Meteor. Mag.*, **33**, 11-35.

Mills, G. A. and R. S. Seaman, 1990: The BMRC regional data assimilation system. *Mon. Wea. Rev.*, **118**, 1217-1237.

Salmon, E. M., and T. T. Warner, 1986: Short-term numerical precipitation forecasts initialized using a diagnosed divergent-wind component. *Mon. Wea. Rev.*, **114**, 2122-2132.

Schlesinger, R. E., 1990: Feedback of deep moist convection to its near environment as diagnosed from three-dimensional numerical model output: Results from an early experiment. *J. Atmos. Sci.*, **47**, 1390-1412.

Tarbell, T. C., T. T. Warner and R. A. Anthes, 1981: An example of the initialization of the divergent wind component in a mesoscale numerical weather prediction model. *Mon. Wea. Rev.*, **109**, 77-95.

Turpeinen, O. M., L. Garand, R. Benoit and M. Roch, 1990: Diabatic initialization of the Canadian regional finite-element (RFE) model using satellite data. Part I: Methodology and application to a winter storm. *Mon. Wea. Rev.*, **118**, 1381-1395.

Wang, W. and T. T. Warner, 1988: Use of four-dimensional data assimilation by newtonian relaxation and latent-heat forcing to improve a mesoscale-model precipitation forecast: A case study. *Mon. Wea. Rev.*, **116**, 2593-2613.

Wergen, W., 1988: The diabetic ECMWF normal mode initialization scheme. *Beitr. Phys. Atmosph.*, **61**, 274-302.

Preprints, Sixth Conference on Satellite Meteorology and Oceanography, Atlanta, GA, Jan 5-10, American Meteorological Society, 313-316.

PHYSICAL RETRIEVAL OF PRECIPITATION WATER CONTENTS USING MULTISENSOR MICROWAVE DATA AND MODEL CONSTRAINTS

William S. Olson and William H. Raymond

CIMSS / Space Science and Engineering Center
University of Wisconsin
Madison, Wisconsin

1. INTRODUCTION

The retrieval of precipitation distributions by passive microwave techniques has been an area of study in satellite remote sensing for well over a decade. The recent initiative to estimate both the horizontal and vertical distributions of precipitating liquid water in the tropics (i.e. the Tropical Rainfall Measuring Mission or TRMM) has further stimulated interest in this area; see Simpson, et al. (1988). The proposed TRMM satellite will carry a suite of sensors including passive and active microwave instruments, as well as visible and infrared radiometers. A combination of microwave and visible/IR sensors has also been proposed for one of the Earth Observing System (EOS) platforms for the purpose of retrieving rainfall rates and other geophysical parameters; ref. Murphy (1987). Methods for determining precipitation distributions based upon data from several instruments having different spectral and resolution characteristics will therefore be required.

Currently multispectral microwave observations from the Special Sensor Microwave/Imager (SSM/I), borne by the DMSP-F8, have provided researchers with the means for retrieving rainfall rates; see Hollinger (1991), Kummerow and Liberti (1990), Petty and Katsaros (1990). The SSM/I is a multichannel, dual-polarization, passive microwave radiometer with channels at 19.35, 22.235, 37, and 85.5 GHz. The diffraction limitation of the SSM/I antenna causes the spatial resolution of measurements to increase with frequency, such that the minimum footprint dimension decreases from 43 km at 19.35 GHz to 13 km at 85.5 GHz. The DMSP also carries the Special Sensor Microwave/Temperature sounder with channels at 50.5, 53.2, 54.35, 54.9, 58.4, 58.825, and 59.4 GHz, and a footprint dimension of approximately 180 km at nadir view. In the present study, a physical retrieval method for estimating precipitation water distributions and other geophysical parameters based upon measurements from the DMSP-F8 SSM/I is developed. Three unique features of the retrieval method are (1) sensor antenna functions are explicitly included to accommodate varying channel resolution, (2) an embedded one-dimensional cloud model is utilized to generate vertical distributions of precipitating and nonprecipitating water, and (3) spectral solutions are sought for certain background parameters, such as humidity, which vary more slowly in the horizontal than the cloud and precipitation water contents. The general framework of the method will allow us to incorporate measurements from the SSM/T and geostationary infrared measurements, as well as information from conventional sources (e.g. radiosondes) or numerical forecast model fields.

2. RETRIEVAL METHOD

The basis of the retrieval method is the minimum variance solution as described in Lorenc (1986). An error functional which expresses the deviation of the observed satellite antenna temperatures from model-derived values, plus an additional constraint which represents the deviation of retrieved geophysical parameters from *a priori* estimates, is derived.

$$E = (TA_{obs} - TA(P)_{mod})^T \Sigma^{-1} (TA_{obs} - TA(P)_{mod}) + (P - P_{apriori})^T \Delta^{-1} (P - P_{apriori}) \quad (1)$$

Here, TA_{obs} is a vector of antenna temperature measurements, $TA(P)_{mod}$ are antenna temperature estimates based on a physical model, P is a vector of geophysical parameters to be retrieved, and $P_{apriori}$ are estimates of the parameters based upon *a priori* knowledge. Σ and Δ are covariance matrices representing observational plus model errors (Σ), and errors in the *a priori* estimates (Δ). In this study all off-diagonal elements of these matrices are neglected.

The antenna temperature model, $TA(P)_{mod}$, embodies the physical relationship between the geophysical parameters to be retrieved and the antenna temperatures measured by the radiometer. An element of $TA(P)_{mod}$ may be written

$$TA(P)_p = A_c^T TB(P)_p + A_x^T TB(P)_{p'} + \delta_p Tbb, \quad (2)$$

where A_c and A_x are the co- and cross-polarized antenna patterns of the radiometer, $TB(P)_p$ and $TB(P)_{p'}$ are the modeled brightness temperatures in the polarization p and orthogonal polarization p' with respect to the plane of polarization of the measurement, and δ_p is the fraction of the radiometer feedhorn pattern not subtended by the antenna. Tbb is the cosmic background radiance (2.7 K). Thus each antenna temperature is modeled as the convolution of the upwelling brightness temperature field by the antenna response pattern of the sensor. In this way, measurements at different channel frequencies or from different sensors which have different sampling / spatial resolution can be accommodated.

The retrieval of preciptation liquid water contents and other geophysical parameters is accomplished by iteratively perturbing the geophysical parameters until the error functional Eq. (1) is minimized. Unlike Lorenc (1986), we minimize the error functional using the memoryless, quasi-Newton method described by Shanno (1978).

3. SENSOR RESPONSE MODEL

In this section, the components of the sensor antenna temperature model, Eq. (2), are described.

3.1 Model Grid

Both the antenna response functions and brightness temperature fields are discretized on a model grid. Rectangular grid "boxes" are defined on the grid, such that the center of each box coincides with the earth location of an all-channel antenna temperature measurement from the SSM/I. The boxes are oriented along the SSM/I A-scans (which contain the all-channel measurements) at a regular spacing of 25 km. Since

the cross-scan separation of succeeding A-scan lines varies along the scan line, the cross-scan dimension of the grid boxes also varies, with a maximum dimension of 25 km in the center of the swath, and decreasing towards swath edge. In the discretization of the antenna response functions and brightness temperature fields, the variation of the grid box dimension with scan position is taken into account.

3.2 Antenna Response Functions

Measurements of the SSM/I antenna reponse functions and a detailed description of the SSM/I scan geometry were provided by Gene Poe (currently with Aerojet Electrosystems Co.). Using this information the integrated co- and cross-polarized antenna responses over each grid box for all SSM/I measurements are computed.

3.3 Radiative Transfer / Cloud Model

The model for the average polarized brightness temperature, $TB(P)_p$, upwelling from a grid box is described here. The earth's surface is characterized by a skin temperature and an emissivity. The emissivity in each polarization is represented using the two-parameter formula of Grody (1988). The downwelling brightness at the top of the atmosphere is set equal to the cosmic background value (2.7 K).

The model atmosphere is divided into 50 mb layers, starting from an assumed top of the atmosphere at 100 mb. Atmospheric temperature falls off linearly with height at a fixed lapse rate of 5.4 K/km from a variable surface value. The surface relative humidity (and the associated water vapor density) is also allowed to vary in the retrieval. It is assumed that the water vapor density falls off exponentially with height, with a scale height of 2.0 km. The temperature lapse rate and vapor scale height reflect the tropical climatological values compiled by Jordan (1958).

Clouds are assumed to occupy a variable cloud fraction within each grid box. Within the cloud fraction, the vertical profiles of precipitating liquid water and ice hydrometeors, as well as nonprecipitating cloud droplets and ice, are determined using a one-dimensional, steady-state cloud model. The updraft in the cloud model is an adaptation of the plume model described in Anthes (1977), which utilizes the water substance conservation equations of Kessler (1965). In light of the arguments by Schlesinger (1990), the rate of accretion of cloud water by rain drops is reduced by a factor of three from the original formulation in Kessler. For a given cloud

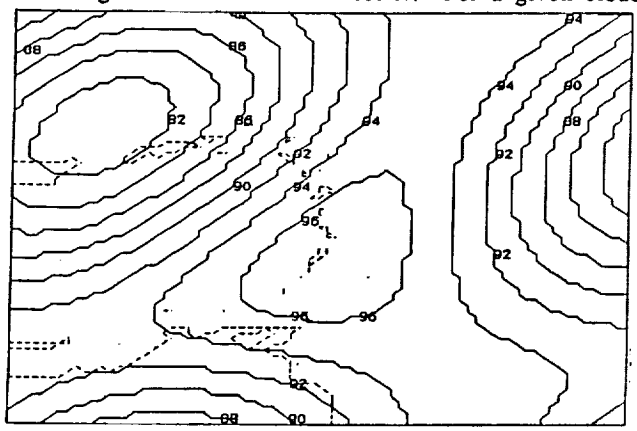

Fig. 1. Retrieved surface relative humidity field in the vicinity of Emily at 10 UTC on September 21, 1987. Values are in percent; coastlines are dashed.

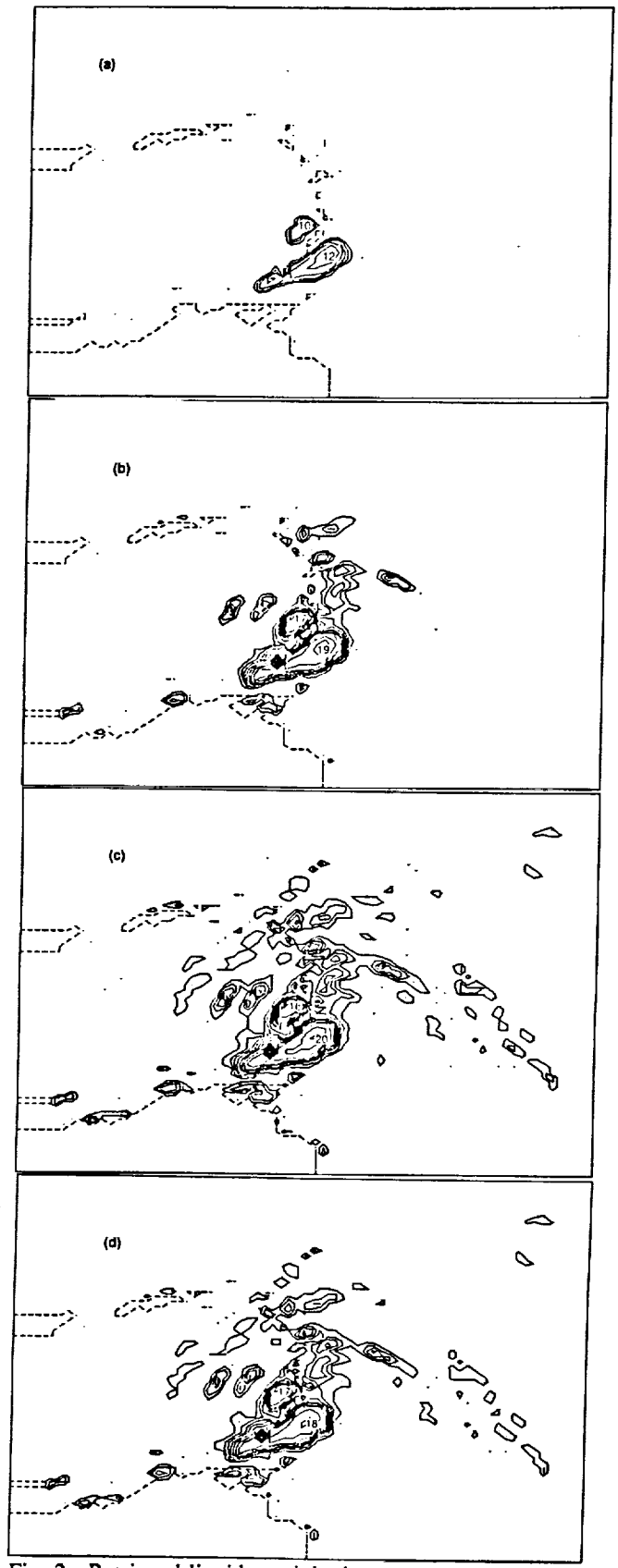

Fig. 2. Retrieved liquid precipitation water contents in the vicinity of Emily at 10 UTC on September 21, 1987. Fields are shown at pressure levels of (a) 550 mb, (b) 700 mb, (c) 850 mb, and (d) at the surface. Contours are drawn at increments of 0.2 g/m^3, starting with a minimum contour of 0.2 g/m^3. Maximum values are in tenths of a g/m^3; coastlines are dashed.

Lorenc, A.C., 1986: Analysis methods for numerical weather prediction. Quart. J. R. Met. Soc., 112, 1177-1194.

Murphy, R. (ed.), 1987: HMMR High-Resolution Multifrequency Microwave Radiometer Instrument Panel Report, National Aeronautics and Space Administration, 59 pp.

Petty, G.W., and K.B. Katsaros, 1990: New geophysical algorithms for the Special Sensor Microwave Imager. Fifth International Conference on Satellite Meteorology and Oceanography, September 3-7, London, England, 247-251.

Schlesinger, R.E., 1990: Feedback of deep moist convection to its near environment as diagnosed from three-dimensional numerical model output: Results from an early experiment. J. Atmos. Sci., 47, 1390-1412.

Shanno, D.F., 1978: Conjugate gradient methods with inexact searches. Math. Oper. Res., 3, 244-256.

Short, D.A., 1988: A statistical-physical interpretation of ESMR-5 brightness temperatures over the GATE area. In Tropical Rainfall Measurements, Proceedings of the International Symposium on Tropical Precipitation Measurements, Tokyo. A. Deepak Publishing, Hampton, Virginia.

Simpson, J., R.F. Adler, G.R. North, 1988: A proposed Tropical Rainfall Measuring Mission (TRMM) Satellite. Bull. Amer. Met. Soc., 69, 278-295.

Simpson, J., and V. Wiggert, 1969: Models of precipitating cumulus towers. Mon. Wea. Rev., 97, 471-489.

Abstrasts, Fourth International Conference on Precipitation, Iowa City, Iowa, April 26-28.

SSM/I Physical Retrieval of Precipitation Distributions and Numerical Model Forecast Applications

William S. Olson and William H. Raymond

CIMSS/Space Science and Engineering Center,
University of Wisconsin, Madison, Wisconsin 53706

The Special Sensor Microwave/Imager (SSM/I) is a passive microwave radiometer with channels at 19.35, 22.235, 37, and 85.5 GHz. At the lower three frequencies, absorption and re-emission of microwaves by liquid precipitation produces a measurable signal which is strongly related to the vertically-integrated liquid water within the radiometer field of view. At 85.5 GHz, liquid precipitation also has an absorption/emission signature, but the upwelling microwave radiances are strongly modulated by scattering off precipitation-sized ice particles which occur at greater altitudes. The combination of channels can therefore be utilized to infer approximate vertical distributions of precipitation water contents.

A physical retrieval method based upon a minimum variance estimator is applied to the SSM/I measured radiances to deduce the vertical distributions of precipitation water contents in different weather systems. The retrieval method incorporates a radiative parameterization for computing upwelling microwave radiances at the SSM/I frequencies as functions of the non-homogeneous distributions of precipitating liquid and ice hydrometeors over a 25 km x 25 km area (the sampling resolution of the SSM/I). The radiative parameterization is based upon detailed calculations of the propagation of microwaves through simulated cloud fields. Both convective and stratiform cloud fields are generated using a numerical model. The spatially inhomogeneous response of the SSM/I instrument to the upwelling radiance field (an antenna diffraction effect) is also explicitly modeled in the physical retrieval method.

Retrieved precipitation water distributions are compared to volume radar scans from Darwin, Australia and Kwajalein, Marshall Islands.

Latent heating rates inferred from SSM/I retrieved precipitation water distributions can be assimilated into numerical weather prediction model forecasts. This kind of information is especially important in data-sparse regions (i.e., over the oceans) where the development of new storms may not be captured by the traditional observational network. Latent heating fields have been assimilated into CIMSS Subsynoptic Scale Model forecasts using a new method, and have shown significant impact on the "spin-up" and subsequent evolution of rapidly deepening storms.

Latent heating information is used in the model's diabatic initialization and in the Newtonian nudging of the temperature field early in the model forecast. The nudging commences with the initial guess and is modified through time by the forecasted wind field

and condensation rates. The Newtonian nudging of the model temperature field at locations experiencing latent heating represents an external forcing that enhances rapid deepening in model forecasts. Our findings show that diabatic initialization using two vertical modes gives a small response, while four vertical modes can produce large changes that on occasion generate model instability. Important factors influencing the outcome include the model grid size, mesoscale content of the initial model fields and the model physics. By introducing an estimated latent heating field into a numerical simulation of the ERICA IOP-5 storm, 24 hour forecasts of central pressure decreased as much as 20 mb.

Preprints, 26th International Conference on Radar Meteorology, Norman, Oklahoma, 24-28 May 1993.

SIMULATION OF SSM/I OBSERVATIONS OF TROPICAL PRECIPITATION BASED UPON DARWIN RADAR DATA

William S. Olson

CIMSS/SSEC, University of Wisconsin
Madison, Wisconsin 53706

Matthias Steiner

Department of Atmospheric Sciences, AK-40
University of Washington, Seattle, Washington 98195

1. INTRODUCTION

In the physical retrieval of precipitation amounts using the satellite-borne Special Sensor Microwave/Imager (SSM/I), an accurate radiative transfer model relating liquid and ice-phase precipitation water contents to upwelling, cloud top radiances is required. One such model that has been used to retrieve precipitation amounts from SSM/I (ref. Olson and Raymond, 1992) is based upon Eddington's second approximation, which includes the effect of multiple scattering of microwave radiances off precipitating hydrometeors. In the present study radar-derived hydrometeor distributions will serve as input to this radiative transfer model, to determine whether or not consistency between the model-output radiances and SSM/I observations can be achieved, and under what modeling assumptions. This study should lead to an improved radiative model and more accurate SSM/I physical retrievals.

2. RADAR DATA AND PROCESSING

Volume radar reflectivity data from the 5-cm Darwin/TOGA installation recorded during the passage of a squall line at 18:20 UTC on February 9, 1988 are interpolated to a cartesian grid with dimensions 240 km x 240 km x 18 km. The grid spacings are 2 km in the horizontal and 1.5 km in the vertical. The radar data in elevation/azimuth/range format are interpolated to grid locations based on the method of Mohr and Vaughan (1979).

Within the convective leading edge of the squall line, the fractions of liquid and ice precipitation associated with a measured reflectivity are estimated using the temperature-dependent partitioning scheme of Moss and Johnson (1992). Within the trailing stratiform precipitation region, it is assumed that the radar reflectivity is due entirely to ice-phase hydrometeors above the freezing level, and below the 6 C level the radar reflectivity is due entirely to liquid hydrometeors. A linear transition from ice to liquid between 0 C and 6 C is assumed. This stratiform precipitation partitioning scheme is based upon model simulations of anvil clouds using a one-dimensional version of the Ridout (1991) model. The vertical profile of environmental temperatures is obtained from the Darwin sounding at 22:00 UTC on February 9, 1988.

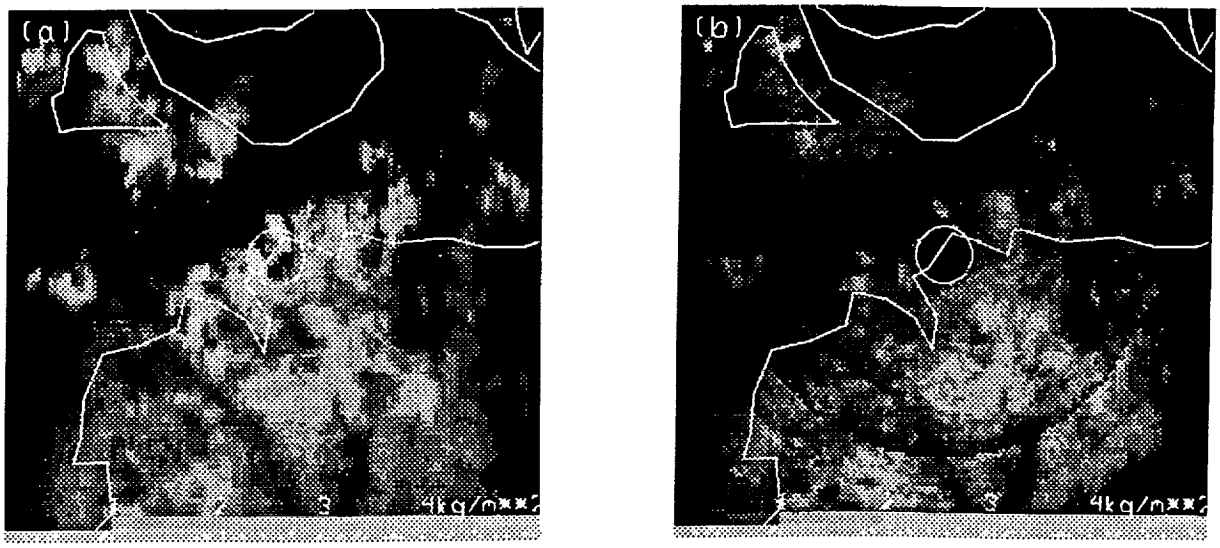

Fig. 1. Fields of slant path-integrated liquid precipitation (a) and ice precipitation (b) derived from the Darwin/TOGA radar at 18:20 UTC on February 9, 1988. Coastlines are indicated by white lines, and the white circle indicates a data-void region in the radar volume scan. Each panel covers an area of 240 km x 240 km.

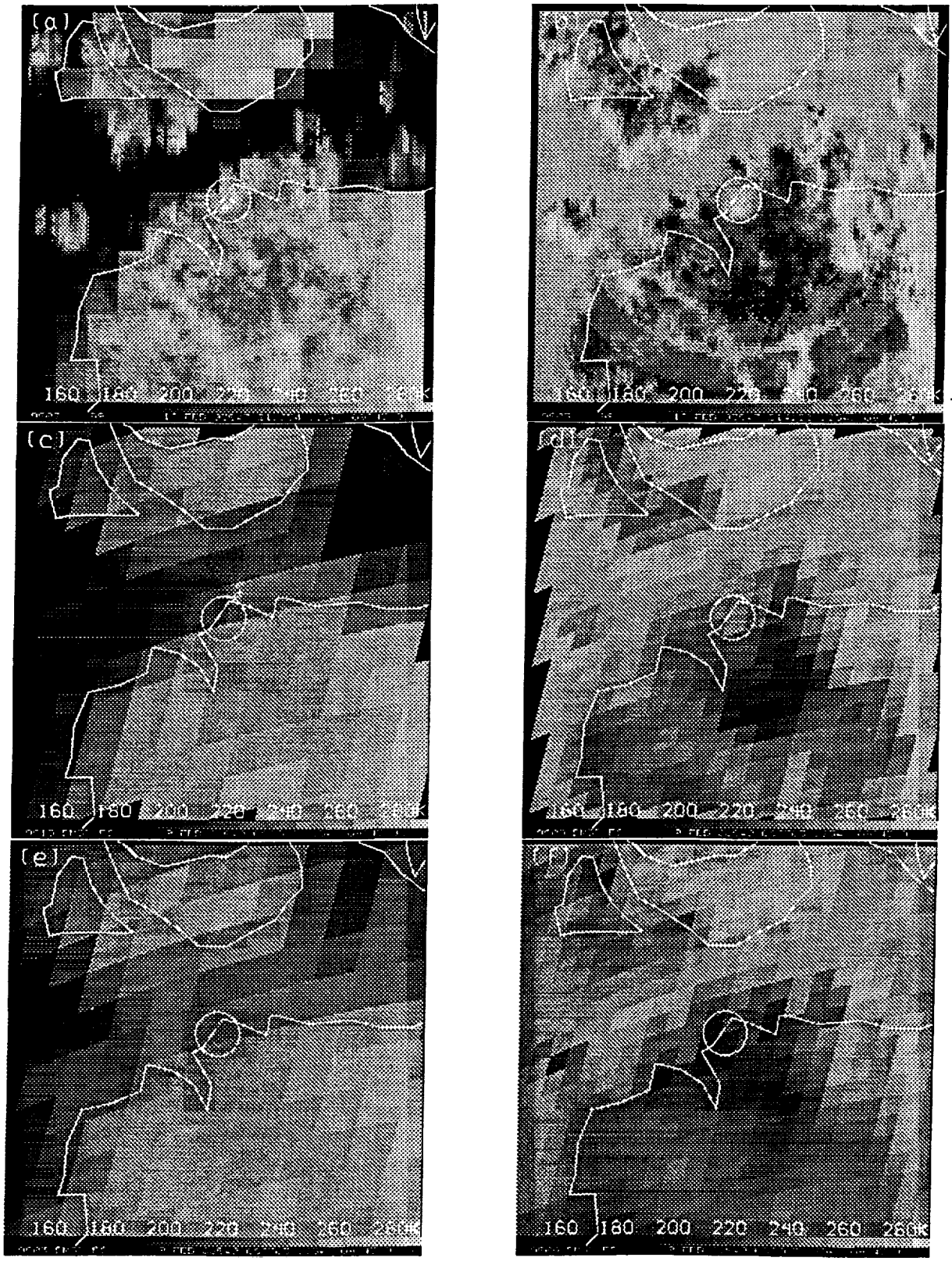

Fig. 2. Simulated brightness temperature fields at 37 GHz and 85.5 GHz are shown in panels (a) and (b), respectively. Simulated antenna temperature fields at 37 GHz and 85.5 GHz are shown in panels (c) and (d), while SSM/I observed antenna temperatures at 37 GHz and 85.5 GHz are shown in panels (e) and (f).

Integrated liquid and ice-phase precipitation fields derived from the Darwin volume scan are shown in Figs. 1a and 1b, respectively. The convective leading edge of the squall line is seen crossing the Darwin radar site along the northern coast of Australia. The region of trailing stratiform precipitation is primarily to the south of the leading edge. Northwest of the radar site, convective precipitation between Bathurst and Melville Islands is also observed. The white circle in the precipitation images indicates a data-void zone in the radar volume scan.

3. SSM/I SIMULATIONS

3.1 Radiative Transfer Calculations

The liquid and ice precipitation water contents derived from the radar are converted to values of extinction coefficient, single-scatter albedo, and asymmetry factor at the SSM/I frequencies (19.35, 22.235, 37, and 85.5 GHz) using the parameterizations in Kummerow and Weinman (1988). Absorption coefficients for molecular oxygen and water vapor are computed using the formulae of Liebe (1985). Microwave absorption by non-precipitating clouds is neglected in the present development. A surface skin temperature of 300 K and emissivities characteristic of land and ocean surfaces, where appropriate, are assumed.

The upwelling microwave radiances at the SSM/I frequencies in two orthogonal planes of polarization at an incidence angle of 53.1^{o} are computed using Eddington's second approximation along individual ray paths through the radar volume. The resulting field of microwave brightness temperatures at 2 km resolution at 37 GHz and 85.5 GHz in the horizontal polarization are shown in Figs. 2a and 2b, respectively.

3.2 Sensor Response

The spatial resolution of the SSM/I varies from about 55 km at 19.35 GHz to 14 km at 85.5 GHz, and antenna temperatures are sampled at intervals of 12.5 km at 85 GHz, and at 25 km at all other frequencies. In order to simulate SSM/I resolution effects, the 2 km resolution images in Figs. 2a and 2b are convolved by the SSM/I 37 GHz and 85.5 GHz antenna patterns. The resulting images are then resampled at the SSM/I measurement locations. The final simulated antenna temperature images at 37 GHz and 85.5 GHz are presented in Figs. 2c and 2d, respectively. Coincident antenna temperature measurements from the SSM/I are shown in Figs. 2e and 2f.

4. RESULTS AND DISCUSSION

A general correspondence between precipitation regions in the simulated and observed SSM/I imagery is evident, and the magnitudes of the antenna temperatures are fairly consistent. However, the simulated antenna temperatures in the convective regions tend to be higher than those observed, while minimum simulated antenna temperatures over the stratiform precipitation region tend to be lower than those observed. These differences are most obvious in the 85.5 GHz imagery, for which scattering by precipitation-sized ice particles, and the associated lowering of upwelling radiances, is more pronounced than at 37 GHz. Errors in the partitioning of the liquid and ice precipitation components in the simulations might account for these discrepancies. Also it may be noted that simulated antenna temperatures at 37 GHz over the ocean tend to be somewhat lower than those observed. The lack of nonprecipitating clouds in the simulations might account for less emission and lower antenna temperatures over the low-emissivity ocean background. The sensitivity of simulated antenna temperatures to modeling assumptions will be the subject of future study.

Acknowledgments

The authors wish to thank Tom Keenan for providing the Darwin radiosonde data utilized in this study, and also Robert Houze, Jr. for providing helpful commentary. Gene Poe kindly provided the SSM/I measured antenna patterns. Ken Bywaters assisted in producing the figures in this paper.

5. REFERENCES

Kummerow, C. D., and J. A. Weinman, 1988: Radiative properties of deformed hydrometeors for commonly used passive microwave frequencies. *IEEE Trans. on Geoscience and Remote Sensing*, **26**, 629-638.

Liebe, H. J., 1985: An updated model for millimeter wave propagation in moist air. *Radio Science*, **20**, 1069-1089.

Mohr, C. G., and R. L. Vaughan, 1979: An economical procedure for cartesian interpolation and display of reflectivity factor data in three-dimensional space. *J. Appl. Met.*, **18**, 661-670.

Moss, S. J., and D. W. Johnson, 1992: Aircraft measurements to validate and improve numerical model parameterizations of the ice and water ratios in clouds. Proceedings of the 11th International Conference on Clouds and Precipitation, Montreal, Canada.

Olson, W.S., and W.H. Raymond, 1992: Physical retrieval of precipitation water contents using multisensor microwave data and model constraints. Proceedings of the Sixth Conference on Satellite Meteorology and Oceanography, Atlanta, Georgia, 4 pp.

Ridout, J. A., 1991: A parameterized quasi-five-cylinder convective cloud model and its application to remote sensing of rainfall. Ph.D. thesis, University of Wisconsin-Madison, 278 pp.